Peptide-based targeting of fluorescent zinc sensors to the plasma membrane of live cells

Citation: Radford, Robert J., Wen Chyan, and Stephen J. Lippard. "Peptide-Based Targeting of Fluorescent Zinc Sensors to the Plasma Membrane of Live Cells." Chemical Science 4, no. 8 (2013): 3080. © 2013 Royal Society of Chemistry

As Published: http://dx.doi.org/10.1039/c3sc50974e

Publisher: Royal Society of Chemistry, The

Persistent URL: http://hdl.handle.net/1721.1/95476

Version: Author's final manuscript: final author's manuscript post peer review, without publisher's formatting or copy editing

Published in final edited form as:
Chem Sci. 2013 August 1; 4(8): 3080–3084. doi:10.1039/C3SC50974E.

Peptide-based Targeting of Fluorescent Zinc Sensors to the Plasma Membrane of Live Cells

Robert J. Radford[a], **Wen Chyan**[a], and **Stephen J. Lippard**[*,a]

[a]Department of Chemistry, Massachusetts Institute of Technology, 77 Massachusetts Avenue, Cambridge, Massachusetts 02139

Abstract

Combining fluorescent zinc sensors with the facile syntheses and biological targeting capabilities of peptides, we created green- and blue-emitting probes that, (i) are readily prepared on the solid-phase, (ii) retain the photophysical and zinc-binding properties of the parent sensor, and (iii) can be directed to the extracellular side of plasma membranes in live cells for detection of mobile zinc.

Introduction

Zinc is an essential trace element, typically found in proteins as a structural or catalytic component.[1] A growing body of evidence, however, has established a role for readily exchangeable or "mobile" zinc located within the pancreas,[2] prostate,[3] and central nervous system.[4] Although the importance of mobile zinc in human health has been extensively documented,[4a,5] knowledge of its physiology and pathology remain incomplete, owing in part to the difficulty in monitoring changes in zinc concentrations at defined cellular locales.[6]

Fluorescent probes are the most common agents for imaging mobile zinc in cells.[6–7] Of the varying classes of fluorescent zinc sensors,[8] small-molecule constructs are the most thoroughly investigated.[6–7] Small-molecule probes can readily diffuse across the plasma membrane, have metal-binding and photophysical properties that can be precisely tuned through chemical synthesis,[6a,7,9] and avoid complex transfection or protein engineering procedures required for protein-based systems.[10] These favourable attributes enable the zinc affinity of small-molecule sensors to be matched to physiological zinc concentrations while using fluorophores that are brighter than fluorescent proteins.[6b,7b] In contrast to their protein counterparts,[10] however, small-molecule probes have unpredictable subcellular distribution, which has led to controversy and confusion within the zinc-sensing community.[11] To address this challenge, we adopted a hybrid approach that integrates the desirable characteristics of small-molecule sensors with peptide scaffolds that are modular, readily synthesized, and biologically compatible. Peptides have previously been used as scaffolds for building zinc sensors[12] and for site-specific delivery of therapeutics,[13] but are unexplored as a means for controlling the localization of fluorescent zinc sensors. The modularity of our constructs enables zinc sensors to be assembled from a plethora of small-

[*]Fax: 1-617-258-8150; Tel: 1-617-253-1892; lippard@mit.edu.

[†]Electronic Supplementary Information (ESI) available: Details regarding the synthesis and characterization of Palm-ZP1 and Palm-ZQ, including additional fluorescence microscopy images are provided. See DOI: 10.1039/b000000x/

[‡‡]The reported apparent $K_{d\text{-}Zn}$ for ZP1 is 0.7 nM in 50 mM PIPES buffer (pH 7), 100 mM KCl. Since we were unable to model the effect of acetonitrile on the CaEDTA/Zn buffering system we compared the zinc affinity of both sensors under identical conditions. See Supplementary Information for more details.

molecule probes[6a] and targeting sequences,[13] facilitating the custom tailoring of sensors to address specific questions in zinc biology. As a proof-of-concept, we report here the synthesis of two plasma membrane targeting constructs, Palm-ZP1 and Palm-ZQ (Figure 1), which deliver two different zinc sensors, ZP1[6a,7b,14] and zinquin,[15] respectively, to the extracellular side of the plasma membrane.

Results and Discussion

Zinc release is essential for the physiology of specialized secretory tissues.[4a,16] Investigating zinc release from cells, however, is challenging due to the difficulty of directing zinc sensors specifically to the plasma membrane. To date, there are only one protein-based[10c] and two small-molecule[17] zinc sensors that localize here. To achieve such targeting, we designed a short peptide consisting of an *N*-terminal palmitoyl group, a 3-residue (~9.8 Å) polyproline helix, two sequential Asp residues, and a *C*-terminal Lys to serve as the point of attachment for the zinc probe (Figure 1). As a defining member of the ZinPyr family of zinc sensors, ZP1[14a] was a logical choice for our first Palm construct. Based on a modified fluorescein core, the ZP family of zinc sensors has binding affinities that span five orders-of-magnitude, a well documented record of zinc-induced turn-on in cells, and members that have carboxylates at the 5- or 6-postion of the fluorescein, which make them amenable for peptide coupling.[7b]

The desired construct, designated Palm-ZP1 (Figure 1a), was designed to localize the zinc-sensing unit to the extracellular side of the plasma membrane. The palmitoyl moiety mimics palmitoylation, a post-translational modification that can direct proteins to the plasma membrane.[18] The polyproline helix provides a rigid spacer,[19] separating ZP1 from surface-bound proteins and bio-molecules that might quench its fluoresence.[20] The two sequential Asp residues provide additional negative charge, which impedes diffusion across the lipid bilayer.[17] Finally, the ε-amino group on the Lys residue serves as a point of attachment for the 6-CO_2H ZP1[14c]

Palm-ZP1 was manually synthesized on Rink amide AM resin by using standard FMOC coupling chemistry. First, the peptide scaffold was constructed by sequential addition of amino acids using published procedures.[21] Next, palmitic acid was coupled to the *N*-terminus under analogous conditions. The acid-sensitive 4-methyltrityl (MTT) protecting group was then selectively removed from the ε-amino moiety on the *C*-terminal Lys,[22] providing a convenient route for "on-resin" incorporation of 6-CO_2H ZP1. Palm-ZP1 was subsequently cleaved from the resin and purified using standard procedures (see Supplementary Information).

To investigate whether the zinc-sensing properties of the ZP1 moiety survived the conditions of solid-phase peptide synthesis (SPPS), we studied the zinc-binding and photophysical properties of Palm-ZP1 in vitro. Because of the hydrophobic palmitoyl moiety,[‡] we used a mixed solvent system consisting of 25 mM PIPES buffer (pH 7) with 50 mM KCl and 50% acetonitrile (v/v). In the absence of zinc, Palm-ZP1 has spectral features that are similar to those of other ZP1 derivatives.[7b] Apo Palm-ZP1 has a λ_{abs} = 517 nm and λ_{em} = 534 nm (Φ_{apo} = 0.16 ± 0.05) (Figure 2, Table S1). Addition of $ZnCl_2$ to a solution of Palm-ZP1 produced a characteristic blue-shift in absorption and emission spectra[7b] (λ_{abs} = 506 nm; λ_{em} = 529 nm) and an enhancement of fluorescence (Φ_{Zn} = 0.79 ± 0.05) (Figure 2). Measurement of the zinc affinity in a CaEDTA buffered solution indicated that the $K_{d\text{-}Zn}$ value of Palm-ZP1 closely approximates that of $K_{d\text{-}Zn}$ of ZP1 (Figure S5 and Table S1).[‡]

[‡]Although apo Palm-derivatives were souble in buffer under concentrations tested (≤ 10 μM), some soluble aggregates were observed upon the addition of $ZnCl_2$.

To assess whether Palm-ZP1 could function in the context of a cellular environment, we conducted live cell imaging experiments. HeLa cells were coincubated in dye- and serum-free Dul-becco's Modified Eagle Media (DMEM) with 2.5 μM Palm-ZP1 and 2.5 μg/L Cell Mask Orange for 15 min (37° C, 5% CO_2) prior to imaging. Serum-free media was used to minimize zinc contamination originating from the serum.[23] After incubation, the cells were washed with PBS, fresh dye- and serum-free media was added, and the cells were mounted on the fluorescence microscope. $ZnCl_2$ (50 μM) was added, and images of both Palm-ZP1 and Cell Mask Orange were acquired using multichannel fluorescence microscopy. Qualitatively, both dyes preferentially localize to the plasma membrane (Figure 3) and appear to have good colocalization. Quantitative image analysis corroborated these findings; Palm-ZP1 and Cell Mask Orange strongly co-localize with Pearson's correlation coefficient $r = 0.70 \pm 0.05$.[24]

Next, we evaluated the ability of Palm-ZP1 to respond reversibly to an extracellular zinc source. Initial cell images had minimal Palm-ZP1 emission, consistent with the low quantum yield for the apo form of the sensor (Figure 4a). Upon addition of 50 μM $ZnCl_2$, an ~1.7-fold increase in Palm-ZP1 fluorescence intensity was observed at the peripheral membrane of the cell (Figures 4b, d), in stark contrast to the localization of ZP1 without the peptide moiety (Figure S6). Notably, no exogenous ionophore such as pyrithione was present, suggesting that Palm-ZP1 responds to changes in *extracellular* zinc concentrations. Subsequent addition of 100 μM EDTA, a cell-impermeable chelator,[25] attenuated the fluorescence signal to initial levels within 5 min (Figure 4c, d).

To verify the extracellular location of the ZP1 unit, we added sodium pyrithione, a known zinc ionophore, to live HeLa cells that had been pretreated with Palm-ZP1 and turned-on by addition of 50 μM $ZnCl_2$ to the media. There were no significant changes to the cellular distribution or fluorescence signal intensity (Figures 5 and S7). The ability of EDTA to quench the zinc-induced fluorescence signal combined with the inability of pyrithione to effect an additional fluorescence signal strongly suggest that the zinc sensing moiety of Palm-ZP1 is located extracellularly.

With the localization and zinc responsiveness of Palm-ZP1 established, we evaluated the robustness by which our construct labeled the plasma membrane. An inherent difficulty in working with some plasma membrane dyes is their narrow range of useful imaging lifetime owing to rapid internalization.[26] To determine the practical imaging window of Palm-ZP1, we incubated the sensor with HeLa cells for different time periods (Figures 6 and S8). Palm-ZP1 is retained in the plasma membrane for prolonged periods of time, ~ 2 hr, before eventually being internalized.

Encouraged by the results with Palm-ZP1, we explored the modularity of the Palm construct by changing the zinc-sensing unit. An inherent advantage of a peptide targeting methodology is the modularity of SPPS. Being able to "mix and match" targeting motifs and zinc sensors enables the development of a sensor for a specific biological application without the investment involved in de novo sensor design. As a demonstration, we synthesized Palm-ZQ, which features zinquin appended to the ε-amino group on the Lys residue of the Palm peptide (Figure 1b). Based on a tosylated quinaldine scaffold, zinquin has known zinc-binding and photo-physical properties[15] and a large zinc-specific fluorescence response.[15] Although the inherent dimness (εΦ) of zinquin and its tendency to compartmentalize within cells have dampened enthusiasm for the probe, the sensor is still widely used due to its commercial availability and compatibility with green- and red-emitting probes in multichannel microscopy experiments.

Analogous to Palm-ZP1, Palm-ZQ was prepared manually using standard solid-phase peptide synthesis methodologies (see Supplementary Information for details). The zinc-binding and photophysical properties of Palm-ZQ were examined and found to be similar to those of zinquin and TSQ (6-methoxy-(8-p-toluenesulfonamido)quinoline) (Figure 7, S9 and Table S2).[15a, 15b] In the absence of zinc, Palm-ZQ has two main absorption bands with maxima at λ_{abs} = 244 and 336 nm (Figure 7), and is essentially non-emissive ($\Phi_{apo} \leq 0.005$). Addition of $ZnCl_2$ gives rise to two new features in the absorption spectrum (λ_{abs} = 263 and 360 nm), and a large increase in fluorescence intensity (>100-fold, λ_{em} = 483 nm, $\Phi_{Zn} = 0.36 \pm 0.01$, Figure 7, Table S2).

To assess the ability of Palm-ZQ to report on changes in extracellular zinc concentration, we carried out live cell imaging in normal epithelial prostrate cells (RWPE-1, Figures 8 and S10.) as well as HeLa (Figure S11). RWPE-1 cells were pretreated with a 10 μM solution of Palm-ZQ, which also contained MitoTracker Red as an internal standard (Figure S10). Initial fluorescence images showed virtually no signal originating from the Palm-ZQ (Figure 8a). Addition of 50 μM $ZnCl_2$ resulted in an ~3.7-fold increase in Palm-ZQ intensity localized to the periphery of the cell (Figure 8b). Again, no ionophore was used, suggesting that the zinquin moiety is responding to changes in extracellular zinc levels. The signal returned to near baseline levels upon addition of 100 μM EDTA (Figure 8c, d). As expected, during that same period there was negligible change in the fluorescence intensity of MitoTracker Red (Figure S10).

We note that Palm-ZQ was much more challenging to image than Palm-ZP1. We attribute this difficulty to two competing factors inherent to Palm-ZQ, an increased hydrophobicity of the construct and lower brightness of the zinc probe. Comparing the percentage of acetonitrile (MeCN) necessary to elute the peptides from an analytical C_{18} reverse-phase column, we qualitatively assessed the hydrophobicity of Palm-ZQ and Palm-ZP1. Palm-ZP1 elutes with 66 % MeCN whereas Palm-ZQ requires 91 % MeCN. The increased hydrophobicity of Palm-ZQ decreases its solubility in DMEM, which further exacerbates its brightness compared to that of Palm-ZP1, zinc-bound Palm-ZP1 being ~ 46-times brighter than zinc-bound Palm-ZQ. The dimness of Palm-ZQ means that higher sensor loading (~ 10 μM) is required to obtain an adequate signal-to-noise ratio for fluorescence microscopy images. This combination of lower solubility and brightness translated into Palm-ZQ being a much more difficult probe to image in live cells. Although Palm-ZQ is not as effective in imaging the plasma membrane as Palm-ZP1, the construct does effectively demonstrate the modularity of the Palm system.

Conclusions

Palm-ZP1 and Palm-ZQ represent a new set of green- and blue-emitting plasma membrane targeted zinc-sensors. They demonstrate that optimized small-molecule fluorescent sensors can work with designed peptide scaffolds to target specific cellular locales. Although not every probe is likely to be amenable to this methodology, by capitalizing on the synthetic ease of SPPS, one could envision using the extensive library of reported analyte-specific sensors[6b,27] to direct the cellular localization of probes and avoid the unpredictability of de novo sensor design. From the perspective of zinc-sensing, the capacity to direct small-molecule probes with varying emission wavelengths and zinc affinities to discrete cellular sites has broad implications for addressing the biological roles of mobile zinc through multicolour microscopy,[6a] the consequences of which are currently being investigated in our lab.

Supplementary Material

Refer to Web version on PubMed Central for supplementary material.

Acknowledgments

This work was supported by NIH grant GM065519 from the National Institute of General Medical Sciences.

Notes and references

1. Bertini, I. Biological Inorganic Chemistry: Structure and Reactivity. Sausalito, CA: University Science Books; 2007.
2. Taylor CG. Biometals. 2005; 18:305–312. [PubMed: 16158221]
3. (a) Costello LC, Franklin RB, Feng P. Mitochondrion. 2005; 5:143–153. [PubMed: 16050980] (b) Costello LC, Franklin RB. J. Biol. Inorg. Chem. 2011; 16:3–8. [PubMed: 21140181]
4. (a) Frederickson CJ, Koh JY, Bush AI. Nat. Rev. Neurosci. 2005; 6:449–462. [PubMed: 15891778] (b) Pan E, Zhang XA, Huang Z, Krezel A, Zhao M, Tinberg CE, Lippard SJ, McNamara JO. Neuron. 2011; 71:1116–1126. [PubMed: 21943607]
5. Colvin RA, Holmes WR, Fontaine CP, Maret W. Metallomics. 2010; 2:306–317. [PubMed: 21069178]
6. (a) Pluth MD, Tomat E, Lippard SJ. Annu. Rev. Biochem. 2011; 80:333–355. [PubMed: 21675918] (b) Dean KM, Qin Y, Palmer AE. Biochim. Biophys. Acta. 2012; 1823:1406–1415. [PubMed: 22521452]
7. (a) Domaille DW, Que EL, Chang CJ. Nat. Chem. Biol. 2008; 4:168–175. [PubMed: 18277978] (b) Nolan EM, Lippard SJ. Acc. Chem. Res. 2009; 42:193–203. [PubMed: 18989940]
8. (a) Jiang PJ, Guo ZJ. Coordin Chem. Rev. 2004; 248:205–229.(b) You Y, Tomat E, Hwang K, Atanasijevic T, Nam W, Jasanoff AP, Lippard SJ. Chem Commun. 2010; 46:4139–4141.(c) You Y, Lee s, Kim T, Ohkubo K, Chae WS, Fukuzumi WS, Jhon GJ, Nam W, Lippard SJ. J. Am. Chem. Soc. 2011; 133:18328–18342. [PubMed: 22023085] (d) Woo H, Cho S, Han Y, Chae WS, Ahn DR, You Y, Nam W. J. Am. Chem. Soc. 2013; 135:4771–4787. [PubMed: 23458333]
9. Guo Z, Kim GH, Shin I, Yoon J. Biomaterials. 2012; 33:7818–7827. [PubMed: 22871424]
10. (a) Bozym RA, Thompson RB, Stoddard AK, Fierke CA. ACS Chem. Biol. 2006; 1:103–111. [PubMed: 17163650] (b) Vinkenborg JL, Nicolson TJ, Bellomo EA, Koay MS, Rutter GA, Merkx M. Nat. Methods. 2009; 6:737–740. [PubMed: 19718032] (c) Dittmer PJ, Miranda JG, Gorski JA, Palmer AE. J. Biol. Chem. 2009; 284:16289–16297. [PubMed: 19363034] (d) Tomat E, Lippard SJ. Curr. Opin. Chem. Biol. 2010; 14:225–230. [PubMed: 20097117] (e) Qin Y, Dittmer PJ, Park JG, Jansen KB, Palmer AE. Proc. Natl. Acad. Sci. USA. 2011; 108:7351–7356. [PubMed: 21502528] (f) Park JG, Qin Y, Galati DF, Palmer AE. ACS Chem Biol. 2012; 7:1636–1640. [PubMed: 22850482]
11. (a) Kay AR, Toth K. J. Neurophysiol. 2006; 95:1949–1956. [PubMed: 16319204] (b) Nowakowski A, Petering D. Metallomics. 2012; 4:448–456. [PubMed: 22498931]
12. (a) Godwin HA, Berg JM. J. Am. Chem. Soc. 1996; 118:6514–6515.(b) Walkup GK, Imperiali B. J. Am. Chem. Soc. 1996; 118:3053–3054.(c) Walkup GK, Imperiali B. J. Am. Chem. Soc. 1997; 119:3443–3450.(d) Shults MD, Pearce DA, Imperiali B. J. Am. Chem. Soc. 2003; 125:10591–10597. [PubMed: 12940742]
13. (a) Kratz F, Muller IA, Ryppa C, Warnecke A. ChemMedChem. 2008; 3:20–53. [PubMed: 17963208] (b) Stewart KM, Horton KL, Kelley SO. Org Biomol Chem. 2008; 6:2242–2255. [PubMed: 18563254]
14. (a) Walkup GK, Burdette SC, Lippard SJ, Tsien RY. J. Am. Chem. Soc. 2000; 122:5644–5645.(b) Burdette SC, Walkup GK, Spingler B, Tsien RY, Lippard SJ. J. Am. Chem. Soc. 2001; 123:7831–7841. [PubMed: 11493056] (c) Woodroofe CC, Masalha R, Barnes KR, Frederickson CJ, Lippard SJ. Chem. Biol. 2004; 11:1659–1666. [PubMed: 15610850] (d) Tomat E, Nolan EM, Jaworski J, Lippard SJ. J. Am. Chem. Soc. 2008; 130:15776–15777. [PubMed: 18973293]

15. (a) Fahrni CJ, O'Halloran TV. J. Am. Chem. Soc. 1999; 121:11448–11458.(b) Hendrickson KM, Geue JP, Wyness O, Lincoln SF, Ward AD. J. Am. Chem. Soc. 2003; 125:3889–3895. [PubMed: 12656623] (c) Frederickson C. Sci. STKE. 2003; 2003:pe18. [PubMed: 12746547]
16. Kelleher SL, McCormick NH, Velasquez V, Lopez V. Adv. Nutr. 2011; 2:101–111. [PubMed: 22332039]
17. (a) Iyoshi S, Taki M, Yamamoto Y. Org. Lett. 2011; 13:4558–4561. [PubMed: 21805969] (b) Li D, Chen S, Bellomo EA, Tarasov AI, Kaut C, Rutter GA, Li WH. Proc. Natl. Acad. Sci. USA. 2011; 108:21063–21068. [PubMed: 22160693]
18. Smotrys JE, Linder ME. Annu. Rev. Biochem. 2004; 73:559–587. [PubMed: 15189153]
19. Sahoo H, Roccatano D, Hennig A, Nau WM. J. Am. Chem. Soc. 2007; 129:9762–9772. [PubMed: 17629273]
20. Togashi DM, Szczupak B, Ryder AG, Calvet A, O'Loughlin M. J. Phys. Chem. A. 2009; 113:2757–2767. [PubMed: 19254018]
21. Kirin SI, Noor F, Metzler-Nolte N, Mier W. J. Chem. Educ. 2007; 84:108–111.
22. Bourel L, Carion O, Gras-Masse H, Melnyk O. J. Pept. Sci. 2000; 6:264–270. [PubMed: 10912906]
23. Bozym RA, Chimienti F, Giblin LJ, Gross GW, Korichneva I, Li Y, Libert S, Maret W, Parviz M, Frederickson CJ, Thompson RB. Exp. Biol. Med. 2010; 235:741–750.
24. French AP, Mills S, Swarup R, Bennett MJ, Pridmore TP. Nat. Protoc. 2008; 3:619–628. [PubMed: 18388944]
25. Radford RJ, Lippard SJ. Curr. Opin. Chem. Biol. 2013; 17:129–136. [PubMed: 23478014]
26. Johnson I, Spence MTZ. The Molecular Probes Handbook ed. 11. 2010
27. (a) Chang PV, Bertozzi CR. Chem Commun. 2012; 48:8864–8879.(b) Chan J, Dodani SC, Chang CJ. Nat. Chem. 2012; 4:973–984. [PubMed: 23174976]

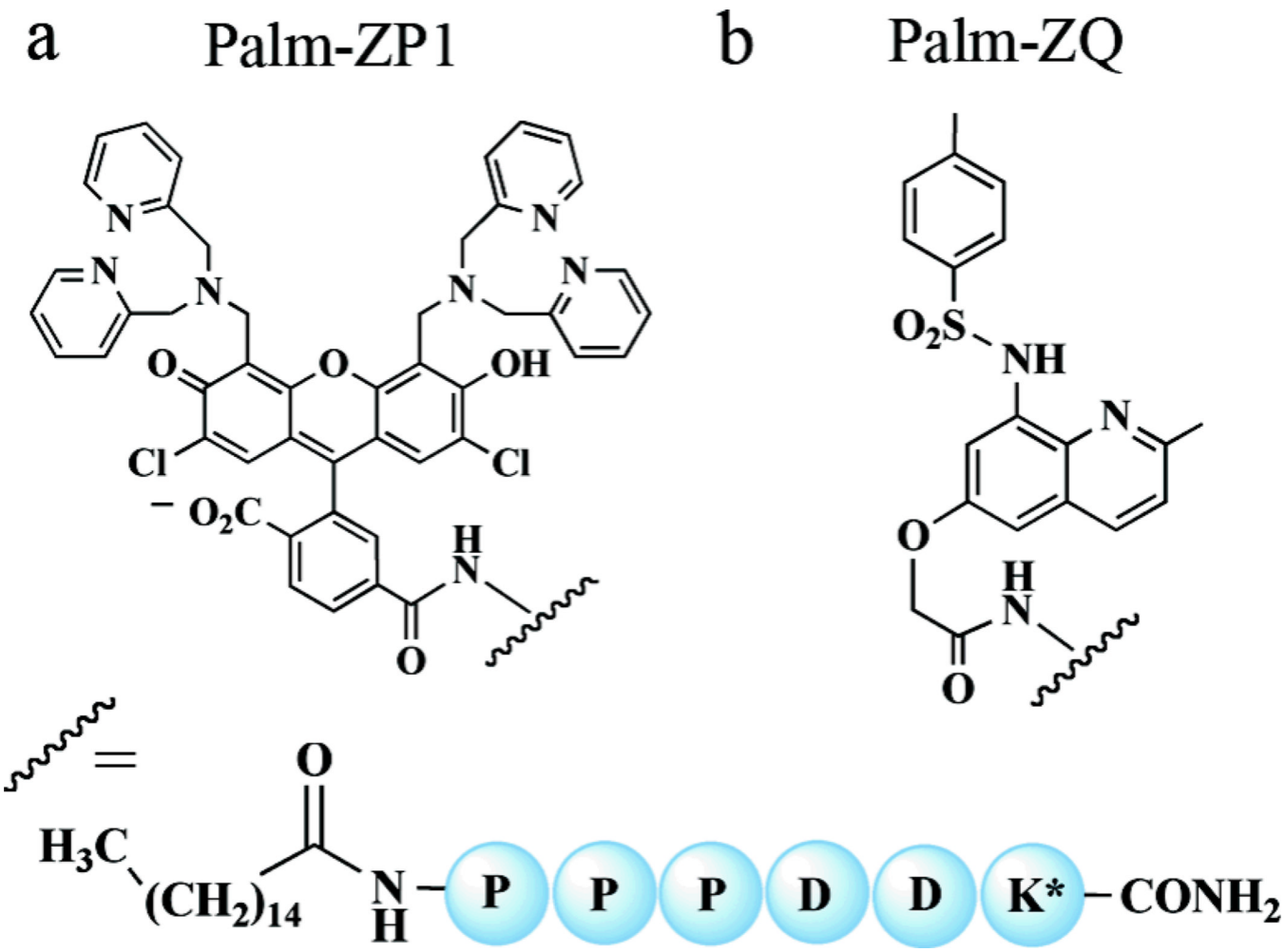

Figure 1.

Illustrations of the two peptide constructs investigated. (a) Palm-ZP1 and (b) Palm-ZQ. Blue circles depict the peptide sequence written from N- to C-terminus. K* indicates the attachment point of the zinc probe, which is to the ε-amino group of the Lys (K) sidechain, and $CONH_2$ represents C-terminal amidation of the peptide.

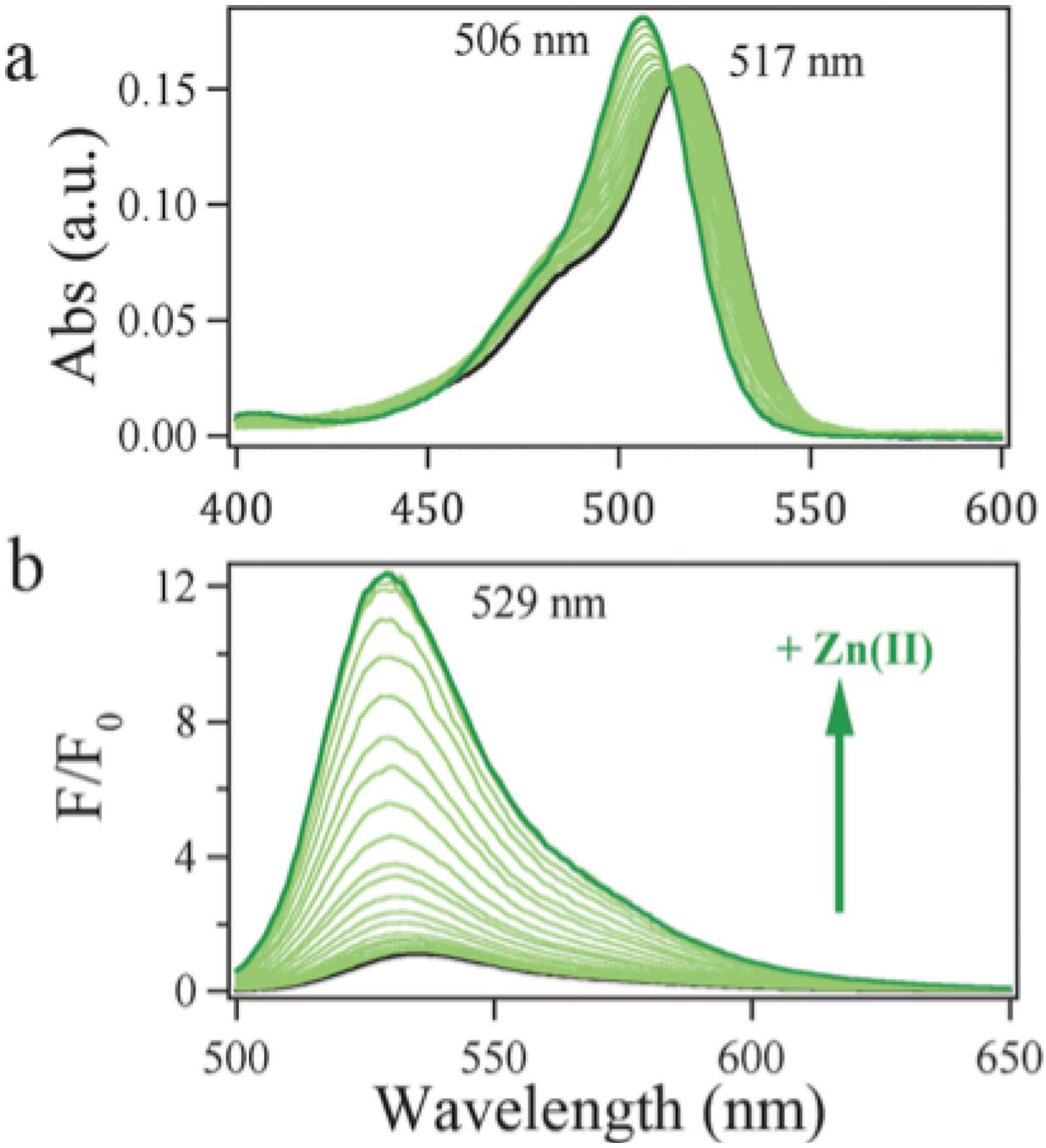

Figure 2.

Changes in the absorption (a) and emission (b) spectra of an ~ 2.3 μM solution of Palm-ZP1 (black) upon addition of successive amounts of $ZnCl_2$ (green). Spectra were acquired in a mixed buffered system consisting of 25 mM PIPES (pH 7) with 50 mM KCl and 50 % (v/v) MeCN.

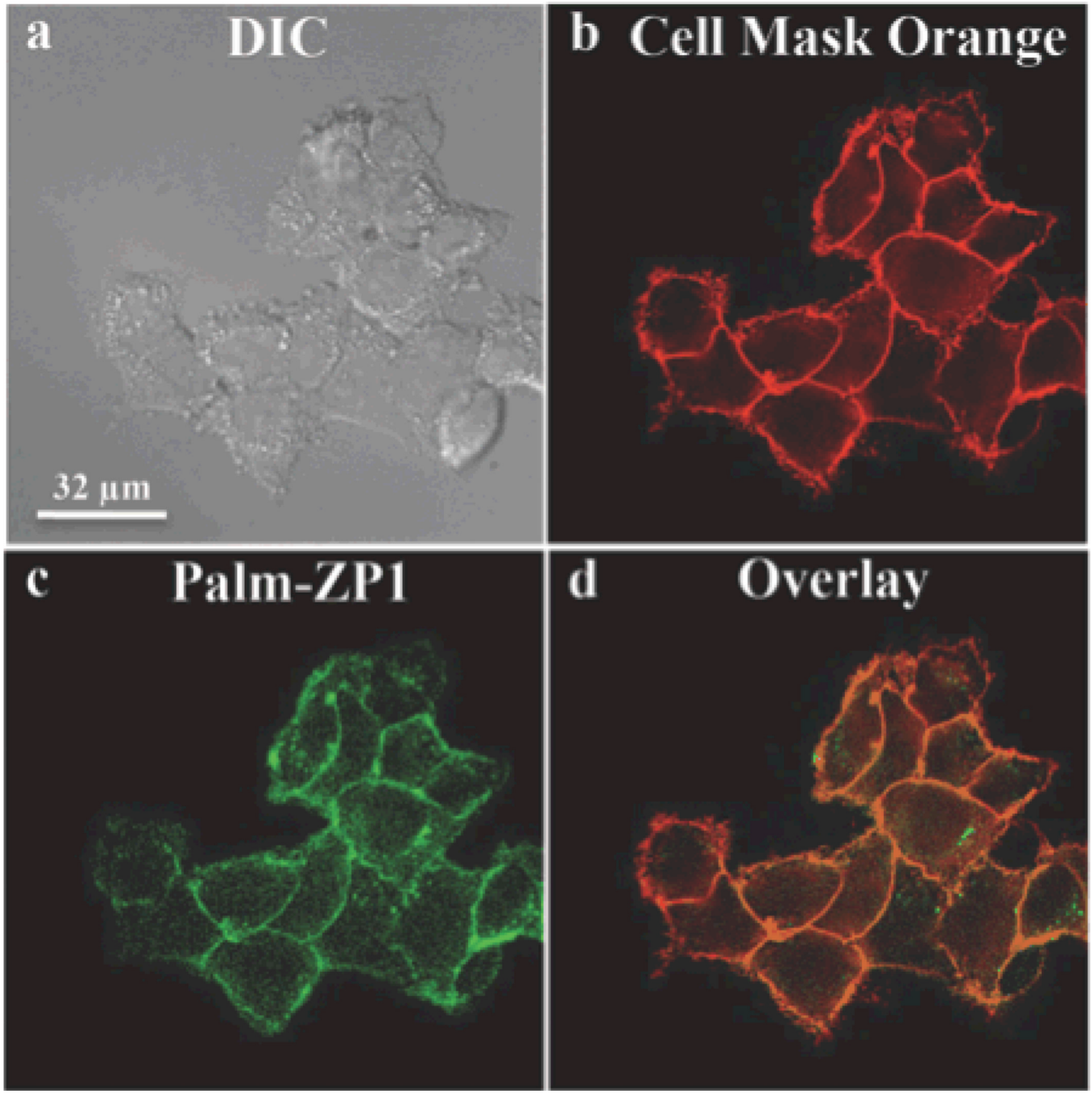

Figure 3.
Localization study of Palm-ZP1 in live HeLa cells. (a) Differential interference contrast (DIC) image. (b) Signal from plasma membrane specific Cell Mask Orange. (c) Signal from zinc-bound Palm-ZP1. (d) Overlay of (b) and (c). Pearson's correlation coefficient r = 0.70 ± 0.05

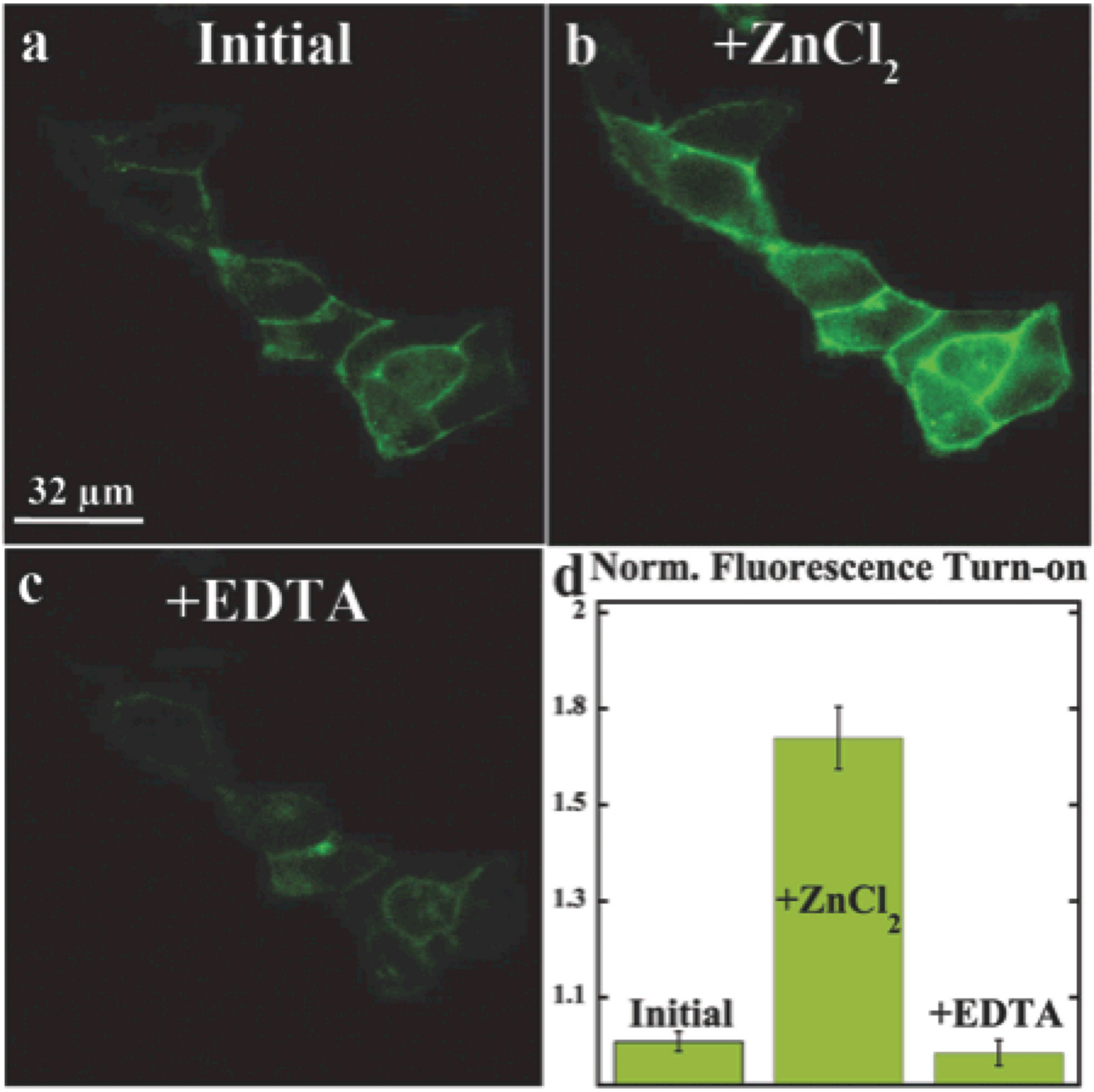

Figure 4.

Zinc response of Palm-ZP1 in fluorescence imaging of live HeLa cells. (a) Initial signal intensity. (b) Emission after addition of 50 μM $ZnCl_2$. (c) Signal after addition of 100 μM EDTA. (d) Average normalized fluorescence signal of Palm-ZP1 during live cell imaging. (n = 18)

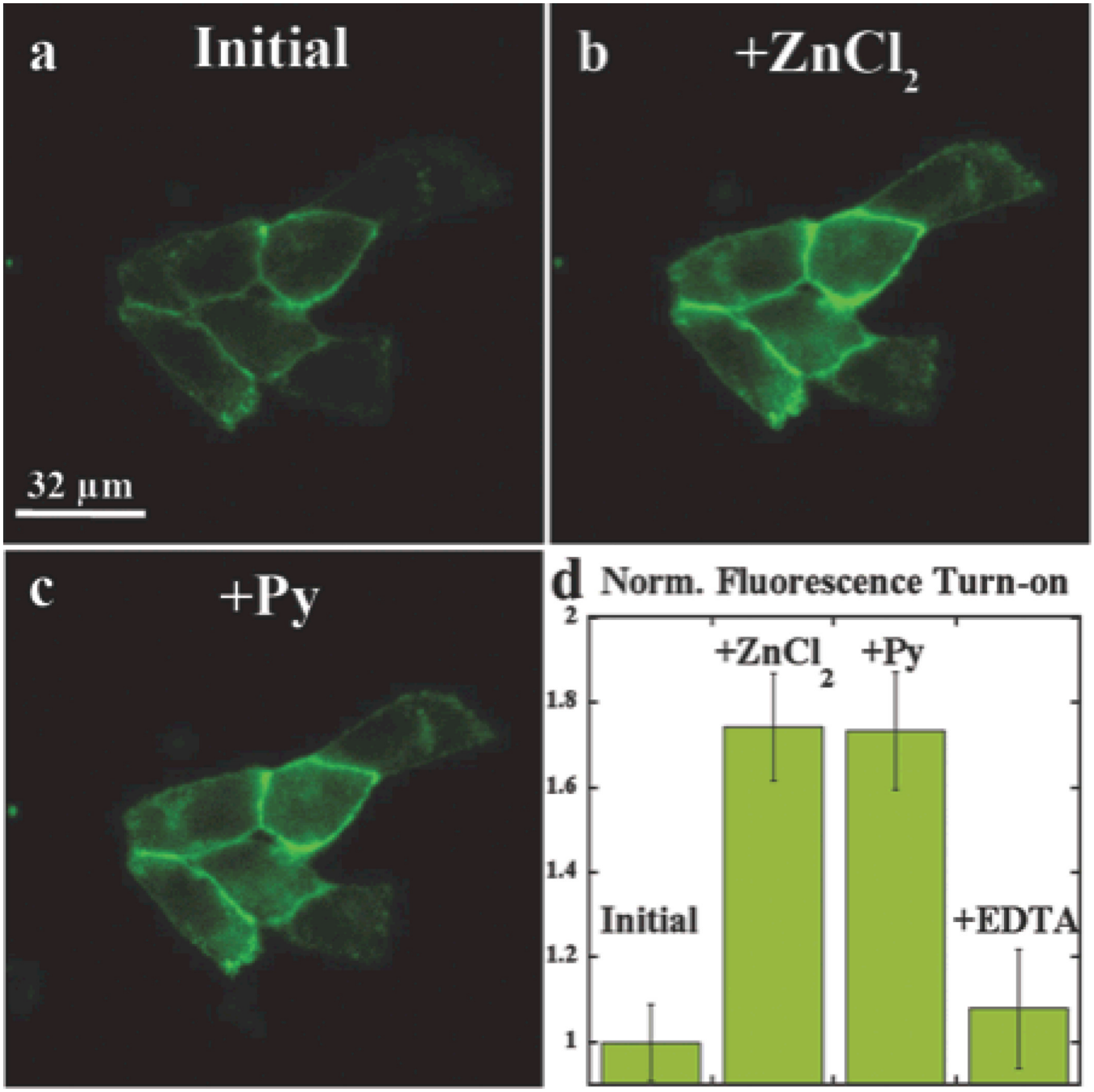

Figure 5.

Fluorescent imaging of Palm-ZP1 in live HeLa cells. The fluorescent signal from Palm-ZP1, (a) initially, (b) after addition of 50 μM $ZnCl_2$, and (c) after addition of 100 μM sodium pyrithione. (d) Quantification of the fluorescent signal from Palm-ZP1 for individual cells in the presence of $ZnCl_2$, Zn/Py (+Py), or EDTA. (n = 12).

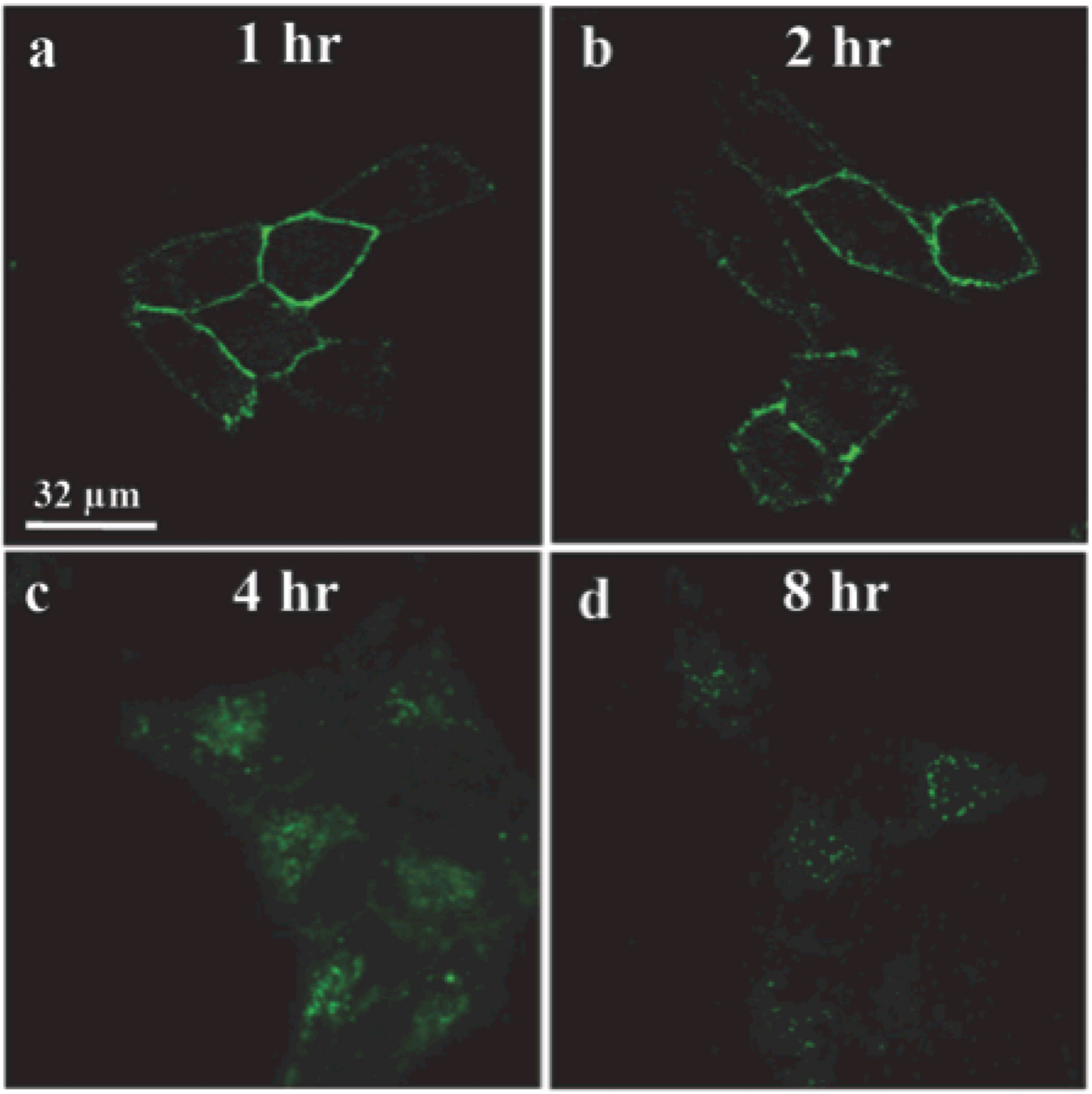

Figure 6.
Location of Palm-ZP1 in live HeLa cells after 1 (a), 2 (b), 4 (c), or 8 hr (d) of incubation at 37 °C and 5 % CO_2. Prior to image acquisition, 50 µM $ZnCl_2$ was added to the cell media to improve signal intensity.

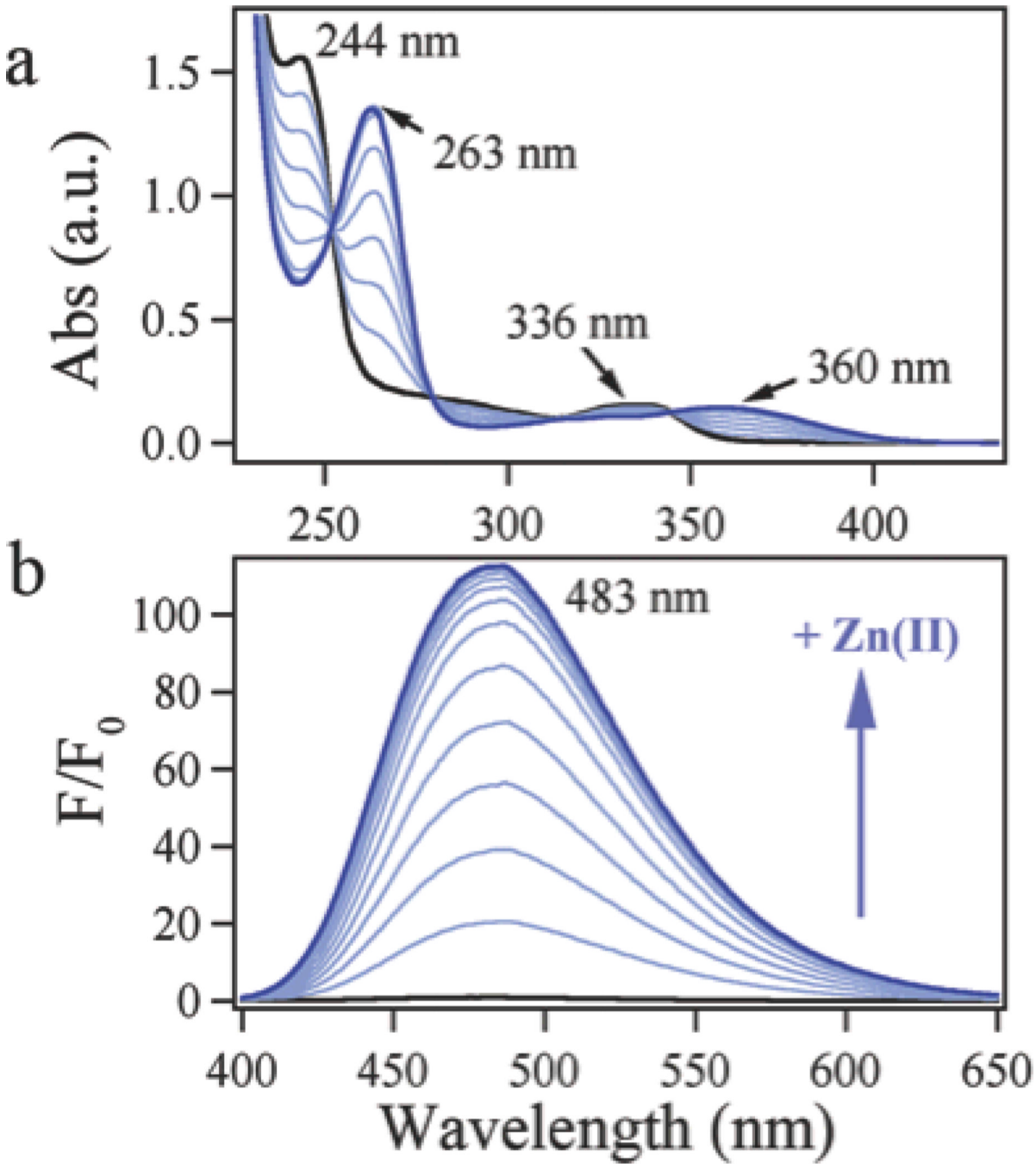

Figure 7.

Changes in the absorption (a) and emission (b) spectra of an ~ 39.5 μM solution of Palm-ZQ (black) upon addition of successive amounts of $ZnCl_2$ (blue). Spectra were acquired in a mixed buffered system consisting of 25 mM PIPES (pH 7) with 50 mM KCl and 50 % (v/v) MeCN.

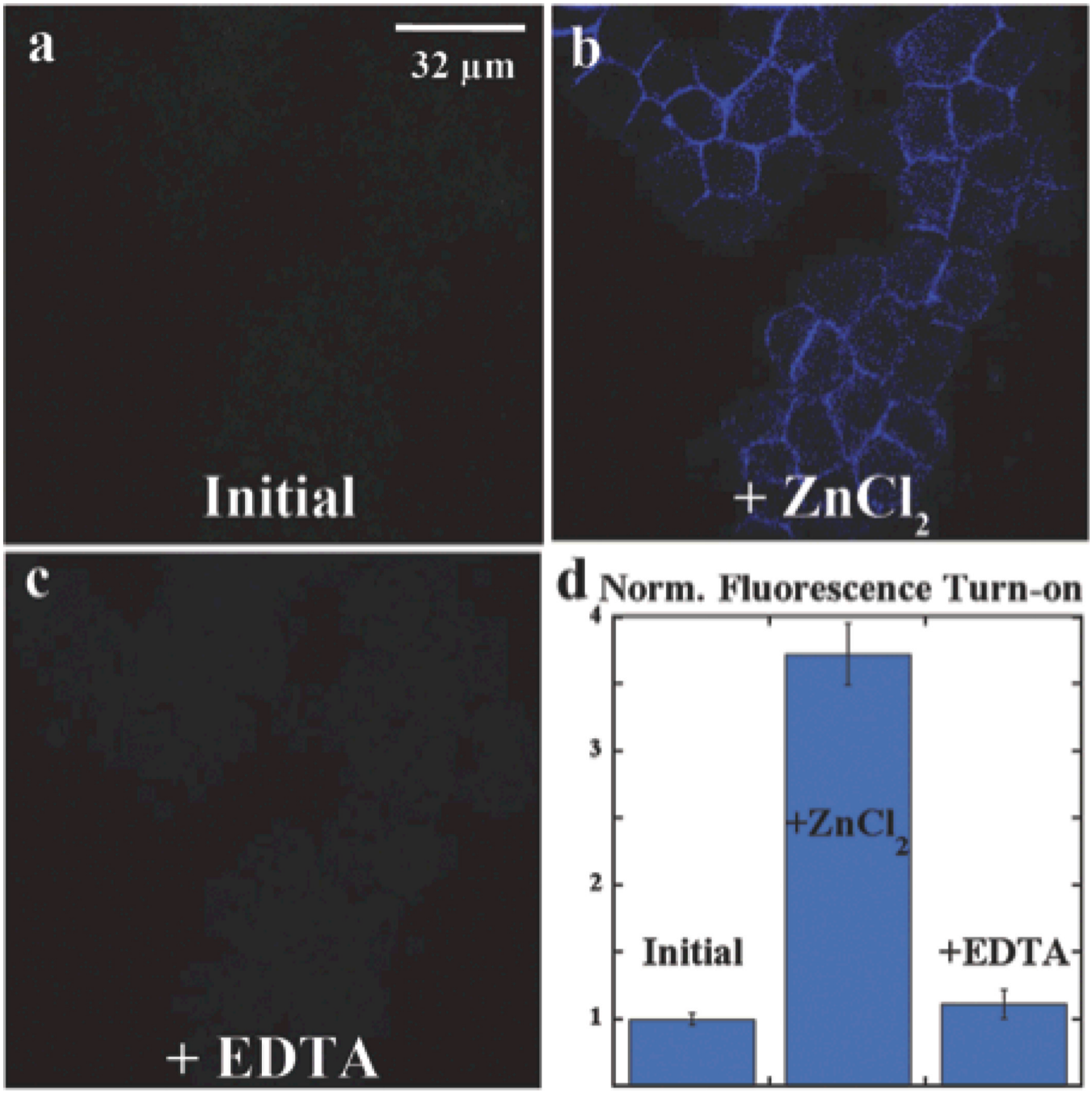

Figure 8.

Zinc response of Palm-ZQ in live cell fluorescence imaging of RWPE-1 cells. (a) Initial signal intensity. (b) Emission after addition of 50 μM $ZnCl_2$. (c) Signal after addition of 100 μM EDTA. (d) Average normalized fluorescence signal of Palm-ZQ during live cell imaging. (n = 20).